

Charge transfer and ionization in low-energy $\text{Ar}^{q+} + \text{Ne}$ collisions

Edson Justiniano, C. L. Cocke, Tom J. Gray, R. D. DuBois,* and C. Can

James R. Macdonald Laboratory and Physics Department, Kansas State University, Manhattan, Kansas 66506

(Received 22 June 1981)

A secondary-ion recoil source was used to study charge transfer and ionization in collisions of Ar^{q+} ($2 \leq q \leq 9$) on Ne at projectile energies between 100 and 1100 eV per projectile charge. Two experimental methods are presented. With the first one we measure cross sections for electron capture by detecting both the initial and final charge states of the Ar ions. With the second method we measure, in addition to those parameters, the charge state of the Ne ions after the reaction. This three-parameter method allows us to distinguish among various competing reaction mechanisms and to measure cross sections for single- and multiple-electron capture, ionization, and transfer ionization. We find that the cross sections for ionization without simultaneous capture are negligibly small, whereas those for transfer ionization are quite important in several cases.

I. INTRODUCTION

The study of electron capture by highly charged ions from both single-electron and multielectron targets has attracted considerable attention over the past few years.¹ Such collision systems are of interest both because of the unusual physics of the slow transfer to the highly charged projectile and because of the importance of such processes in high-temperature plasmas. For example, there is a need for a better understanding of processes that lead to energy losses by tokamak plasmas. One important such process is electron capture from hydrogen by highly charged impurities in the plasma, followed by line radiation from the excited projectile states so formed.² The possible use, in x-ray lasers, of the inverted populations generated by capture to excited states of the projectile brings additional interest to this problem.

While collisions involving atomic hydrogen as a target present the cleanest case for theoretical analysis, the study of collisions involving multielectron targets is nevertheless useful in gaining insight into capture and ionization processes involving low-energy highly charged (LEHQ) projectiles. For example, systematic studies of the dependence of the transfer cross sections on target ionization potential, and of the population of multiply excited states in multielectron transfer, require the use of more complex targets. Salzborn *et al.*³⁻⁵ have made a systematic study of electron capture by LEHQ projectiles in rare-gas-rare-gas collisions at collision energies typically higher than the ones presented here. They found large values for the

cross sections for both single- and multiple-electron capture and found that they followed certain scaling rules. Crandall *et al.*⁶ have reported cross sections for Xe ions on He and Ar targets. More recently, Vane *et al.*⁷ reported total cross sections for capture by recoiling Ne ions from Ne gas. The $\text{Ar}^{2+} + \text{Ne}$ system has been studied in some detail by Huber.⁸ Experimental information on the principal quantum number of the captured electron for very low energy Ne^{q+} and N^{q+} on He, Ne, Ar, H_2 , CH_4 , and NH_3 has been reported by Beyer *et al.*⁹ and Mann *et al.*¹⁰

The cross-section work cited above involved measurement only of the charge change of the projectile, as is the case with the vast majority of capture cross-section work in the literature. There is reason to believe that multiple capture by LEHQ ions may populate excited states on the projectile that promptly autoionize, thus changing the final charge state observed for the projectile. This is a special case of transfer ionization (TI),^{11,12} a process where one or more electrons are ejected from the projectile-target system at the expense of the exoergicity of the capture process. Experimental evidence for the importance of TI in such collisions at higher energies than those considered here has been reported. Flaks *et al.*¹³ studied the total electron production in Ne^{q+} on Xe and Xe^{q+} on Ne ($0 \leq q \leq 4$). Woerlee *et al.*¹⁴ and Ogurtsov *et al.*¹⁵ have observed autoionization lines due to double capture into excited states of the projectile in collisions of multiply charged Ne (and He) ions up to 100 keV ($1 \leq q \leq 4$) with noble gases. At lower energies, similar results have been reported by

Niehaus *et al.*¹¹ and Morgenstern *et al.*¹⁶ for projectiles with ionization state up to three. Groh *et al.*¹⁷ have found evidence for TI in Xe^{q+} -Xe collisions at $q \times 76$ eV/amu.

In this paper we report measurements of cross sections for single- and multiple-electron capture, ionization, and transfer ionization in Ar^{q+} ($2 \leq q \leq 9$) on Ne collisions at impact energies of 100 to 1100 eV per projectile charge. We have previously reported evidence for the importance of TI in $\text{Ar} + (\text{He}, \text{Ne}, \text{Ar}, \text{Xe})$ collisions in a paper which includes a much abbreviated account of some of the data presented here.¹⁸ We have used a secondary-ion recoil source for the production of the LEHQ Ar ions. Two experimental methods for obtaining the cross sections are presented. The first method involves the measurement of the initial and final charge states of the projectile. This provides us with cross sections for single- and multiple-electron capture by the Ar projectiles from the Ne target. The second method measures, besides the two parameters already mentioned, the charge states of the capture-produced Ne ions. This allows us to measure cross sections for direct ionization and TI as well as for normal single and multiple capture, and thus to distinguish among various competing channels through which the reaction can proceed.

II. EXPERIMENT

A. Projectile charge-changing cross sections: Configuration I

The LEHQ ions used in this experiment were produced in a secondary-ion recoil source by bombarding a tenuous gas target with a fast-charged particle beam. The primary collision generates recoil ions with high ionization state and center-of-mass energies typically below 10 eV. These ions are then extracted for use in subsequent collisions. More detailed discussions of the source¹⁹ and of the physics of the primary collision are given elsewhere.²⁰⁻²²

In this experiment (Fig. 1) a pulsed 19-MeV F^{4+} beam from the Kansas State University EN tandem Van de Graaff accelerator was passed through a 0.3–1.0-mTorr Ar gas target. The pressure in the primary cell was measured with a MKS-type 220B Baratron²³ capacitance manometer. The base pressure in the whole scattering chamber was typically 2×10^{-6} Torr. The fast fluorine beam was

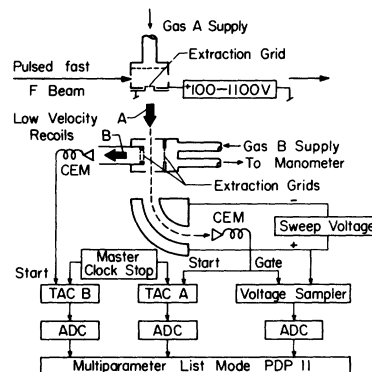


FIG. 1. Schematic of apparatus. The collector for recoils "B" and associated electronics are not used for configuration I experiments (see text).

pulsed to a time width less than 5 ns with a frequency of 125 kHz. The Ar ions thus produced were accelerated out of the collision region by an electric field applied at right angles to the incident "pump" beam and directed through a 2-cm-long secondary gas cell containing Ne gas at pressures between 0.1 and 1.0 mTorr. The entrance and exit apertures of the cell were 1.0 and 2.5 mm in diameter, respectively. The pressure in the secondary cell was read by a MKS-type 90 (Ref. 23) capacitance manometer and automatically stabilized to better than 5% by a servo-assisted gas-handling system.

The time of flight of the Ar ions (TOF-A) from their production until their detection by a channel-electron multiplier (CEM) is proportional to $\sqrt{m/q}$. Therefore, TOFA is a measurement of the initial charge state q of the Ar projectiles, before interaction with the secondary gas target. In Fig. 2 we present an Ar charge-state spectrum from the LEHQ ion source. Contaminant ions from N_2 , O_2 , and H_2O in the source are clearly visible and indeed are somewhat stronger in this spectrum than was the case during most production runs. Background runs were made in order to correct for small contaminations in the Ar peaks, such as O^{2+} in the Ar^{5+} peak.

A double-focusing spherical-sector electrostatic analyzer was used to determine the final charge state q' of the projectiles after interacting with Ne atoms in gas cell B. If the energy E of the Ar incoming projectile is qV_1 and, by interacting with a Ne atom, its charge is changed to q' , the electrostatic analyzer will let this ion pass to detection by the CEM at analyzing voltage V_a such that

$$K \frac{qV_1}{q'} = V_a, \quad (1)$$

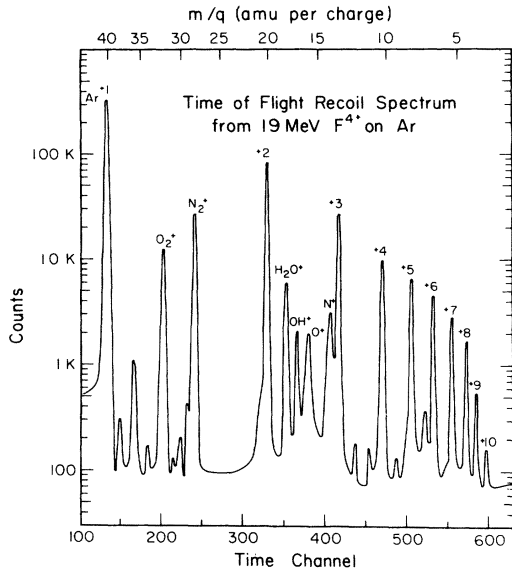


FIG. 2. A singles TOF-A spectrum showing the charge states of Ar yielded by the source.

where K is a constant depending only on the electrostatic analyzer geometry. The voltage V_a was swept repetitively by a triangle wave generator. The value of V_a sampled at the time of detection constitutes a measure of q' . Typically, the voltage V_a was swept from slightly below KV_1 to above $2KV_1$. For each event both the time of flight TOF-A, and the analyzer voltage V_a were recorded by a PDP 11/34 computer with multiparameter data acquisition capabilities. In Fig. 3 we show an example of a two-dimensional spectrum obtained by such a procedure for the case of Ar^{q+} ions incident on Ne at an Ar energy of $500 \text{ eV}/q$. Such a spectrum takes typically 30 min to accumulate at a total singles rate of 10^4 Hz maximum (at $q=q'$) in the TOF-A spectrum. All events that do not involve charge change in the secondary-gas cell occur at $V_a = KV_1$ and are called direct events in Fig. 3. Events where capture of 1, 2, and 3 electrons occur lie on curved loci as shown in that figure.

Absolute cross sections $\sigma_{q,q'}$ for the capture of $(q-q')$ electrons by an Ar^{q+} ion from the Ne target were obtained by the following procedure: We first determined, from the two-dimensional spectrum, corrected yields of the events associated with projectiles of initial charge q and final charge q' according to the expression

$$Y_{qq'}(x) = \frac{N_{qq'} q'}{\epsilon(E) q} \frac{1}{1 + \delta_{qq'}(\tau - 1)}, \quad (2)$$

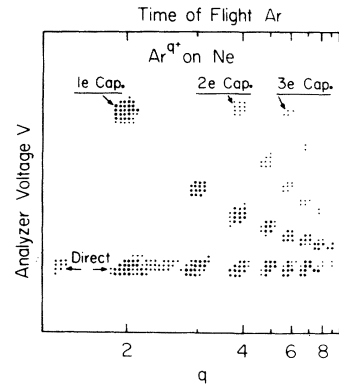


FIG. 3. A two-dimensional spectrum of TOF-A vs V_a . The size of each dot increases with the number of counts in that channel.

where $N_{qq'}$ is the number of raw counts in the two-dimensional spectrum, x is the Ne target thickness, τ is the dead time associated with non-capture events, and $\epsilon(E)$ is the relative CEM efficiency.

Expression (2) incorporates three types of correction to the raw data: (1) The factor (q'/q) arises because the analyzer, whose sweep assigns equal-time durations to equal increments in V_a , spends a time accepting each charge state which is proportional to V_a , and thus, from (1), to q/q' . Thus, for fixed q , lower q' are counted longer in the raw numbers, and this effect must be removed. (2) The dead-time correction factor is necessary since the count rate for $(q=q')$ events was typically quite high (10 kHz) and caused dead times as high as 40% in the event-recording computer. This dead time was measured by recording simultaneously the singles TOF-A spectrum in a one-dimensional fast pulse-height analyzer, whose dead time could be kept below 3%. Comparison of yields from the two analyzers gives τ . This procedure ensures a consistent setting of windows along the TOF-A axis for both direct and charge-exchanged events. The dead time associated with capture events was negligibly small. (3) The factor $\epsilon(E)$ is the relative ion-energy-dependent efficiency of the CEM. This was measured by varying the voltage of the CEM cone, keeping the gain constant, and recording the resultant change in the TOF-A singles spectrum. This efficiency was found to be flat above 3 keV, and, since the cone was run at -1.5 kV , affects only data involving $(q,q') = (2,1)$. The largest correction due to $\epsilon(E)$ was 35% for $\sigma_{2,1}$ at $80 \text{ eV}/q$.

Cross sections were determined in two ways: (1) For small x ,

$$\sigma_{qq'}(x) = [Y_{qq'}(x)/Y_q^T(x)]/x, \quad (3)$$

where the total yield of charge state q in the spectrum is defined as

$$Y_q^T(x) = \sum_{q'} Y_{qq'}(x). \quad (4)$$

Data were recorded only for $q/q' \geq \frac{1}{2}$. Cross sections for lower q/q' are small. In Fig. 4 we show typical pressure dependences obtained at 500 eV/ q . Complete pressure dependence curves up to 1 mTorr were run at 500 and 750 eV/ q and cross sections were extracted from the slopes of the growth curves in the linear regions, typically below 4×10^{-4} Torr. Absolute values of x were calculated from the known pressure from the capacitance manometer and the gas-cell length. (2) Since our data yield a nearly complete network of $\sigma_{q,q'}$ for each q , we may make corrections to the data for multiple collision contributions. Using the network of coupled equations described by Allison,²⁴ we followed an iterative procedure to correct the first order cross sections given by Eq. (3) for double collision contributions. This procedure yielded cross sections independent of x up to 1 mTorr pressure, even when corrections for cases of double and triple charge exchange became as high as 30%. We were thus able to extract cross sections reliably from fixed pressure data at other argon energies. Background pressure runs were made in all cases. Relative errors expected from the data analysis procedure are indicated by typical error bars shown on the data in Fig. 5. Enough independent data points were taken at 500 and 750 eV/ q to assign relative error bars on the basis of the reproducibility

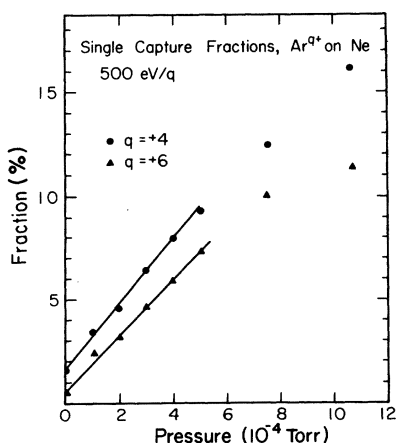


FIG. 4. A plot of the fraction of the initial Ar^{q+} beam undergoing single-electron capture from Ne vs pressure in the secondary cell, for $q = +4$ and $+6$.

of the data. The accuracy of the absolute cross-sections scale is limited by our knowledge of the effective gas-cell length. The difference between the true cell length and the cell length plus aperture diameters is 18%. Since the assumption of neither length appears overwhelmingly compelling to us, we adopted an intermediate value for the cell length of the true length plus the sum of the aperture radii. We have measured cross sections with other cell geometries, and, on the basis of the resulting change in the absolute scale factor, assign an error bar of 15% overall to our absolute scale.

In Figs. 5 and 6 we present cross sections for projectile charge change of one, two, and three charge units, labeled single (p), double (p), and triple (p) capture, respectively. We use the (p) to indicate that only projectile charge states were measured. As we discuss below, the "single, double, triple" designations applied in such a case may be misleading in terms of the physical processes involved. Our absolute cross sections are in rather good agreement with those of Salzborn *et al.*³ at higher energies, and with $\sigma_{2,1}$ of Huber⁸ at our highest energy. At low energies our cross sections go above those of Huber, although barely outside his error bars. We note that this discrepancy would be removed if the $\epsilon(E)$ correction were removed; we can find no justification for doing this, however. In order to check this point, we repeated our measurements of $\sigma_{2,1}$ at low energies using a

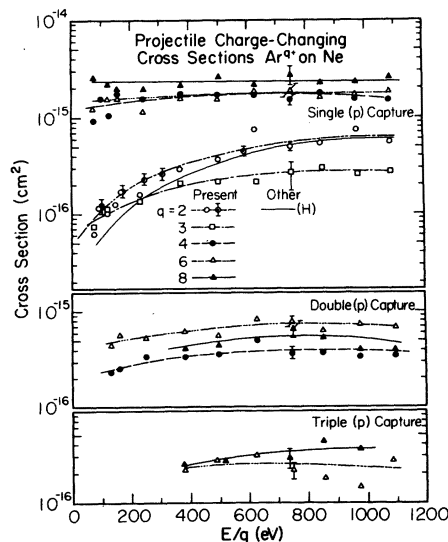
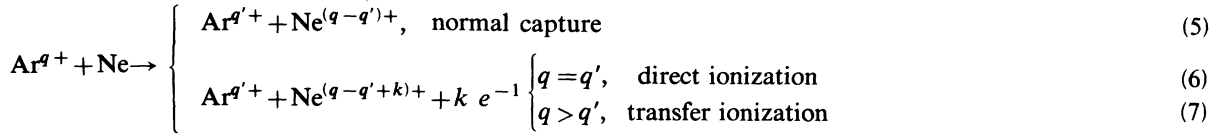


FIG. 5. Energy dependences of projectile charge-changing cross sections (p) for Ar^{q+} on Ne. Data for $q = 5$ and 7 have been omitted for clarity. The previous single-capture experimental curve of Huber (Ref. 8) for $q = 2$ is shown as a solid line.

channel-plate detector whose measured $\epsilon(E)$ was flatter below 3 keV than was that for the CEM. The results, shown as open circles with dots at their centers in Fig. 5, confirmed the results found with the CEM.



are indistinguishable in configuration I experiments. In order to differentiate among these channels experimentally, we installed a second recoil-ion extractor in the secondary gas cell, with a second

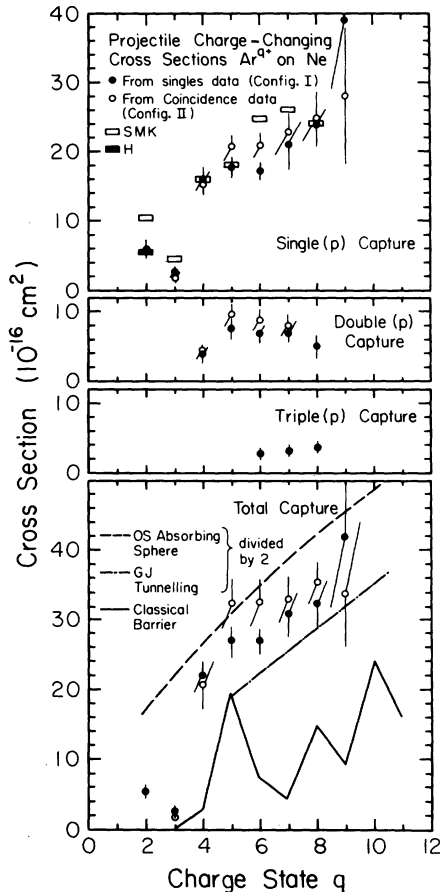


FIG. 6. Projectile charge-changing cross sections (p) from configuration I data are shown as solid circles. Open circles are obtained by summing appropriate partial cross sections from configuration II data. Other experimental points are from Salzborn *et al.* (SMK, Refs. 3–5) and Huber (H, Ref. 8). Theoretical curves for total capture are from Olson and Salop, absorbing sphere, Ref. 27; Grozdanov and Janev, tunneling model, Ref. 29; classical barrier, Refs. 9, 10, and 28.

B. Coincidence measurements: Configuration II

Reactions leading to final state q' of the Ar include those in which ionization of the projectile or target may occur. Thus, processes of the types

CEM to detect the Ne recoils (Fig. 1). The flight time from the secondary collision event to this CEM, TOF- B , is dependent on the Ne charge state. The grid voltages on the B extractor were set at ± 10 V, sufficient to collect the Ne recoils without substantial deflection of the Ar beam. The overall collection efficiency of the B -extractor–CEM combination was measured to be near 10%.

For each event, three parameters were recorded: TOF- A , TOF- B , and V_a . Typical singles rates were 10^4 and 30 Hz in the TOF- A and TOF- B spectra, respectively. Since the addition of the B extractor reduces substantially the overall efficiency of the system, running times up to 12 h were necessary to accumulate sufficient statistics (~ 100 counts for the higher- q coincident events).

In sorting the three-dimensional data, we set appropriate windows in the TOF- A spectrum to isolate one q at a time and obtained plots of TOF- B versus V_a for each q . The former variable determines $(q - q' + k)$, the final Ne charge, and the latter determines (q'/q) , giving the final Ar charge. Such plots are shown in Fig. 7 for 500-eV/ q Ar on Ne and two initial Ar charge states.

Several qualitative features of Fig. 7 deserve discussion. For $q = 4$ [Fig. 7(a)], the major population is on the charge-conservation diagonal, i.e., normal capture [Eq. (5)]. Very few Ne^{1+} ions are observed in coincidence with Ar^{4+} exiting ions, showing direct ionization of the Ne [Eq. (6)] is very weak. Indeed, those few events which are seen in the figure are due to random coincidences between Ar^{4+} ions and Ne^{1+} recoils from uncorrelated events. A quantitative measurement of the randoms was performed separately by displacing the TOF- B spectrum in time by $8 \mu\text{s}$. Randoms were subtracted in the calculation of cross sections from these data. They typically contributed less than 1% of the reals in regions of the spectrum other than the $q = q'$ line.

For $q = 7$ [Fig. 7(b)], the picture is substantially different. While direct ionization remains weak,

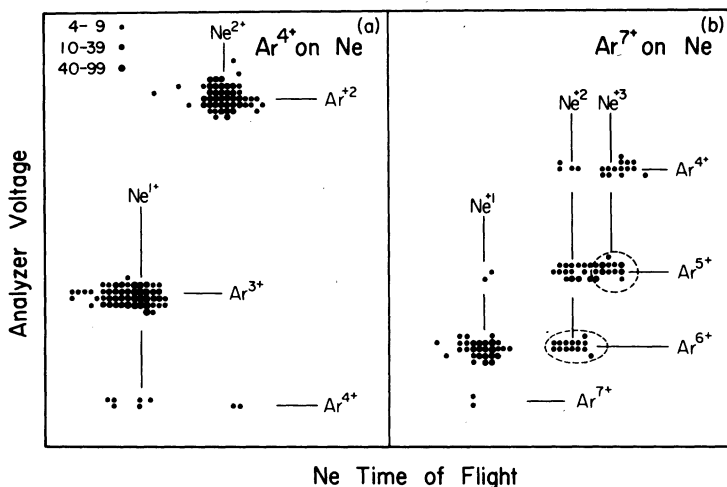


FIG. 7. Two-dimensional slices of configuration II data for (a) Ar^{4+} and (b) Ar^{7+} on Ne showing TOF- B vs V_a . Final charge states of Ar and Ne are dispersed vertically and horizontally, respectively, and are labeled in the figure. Dashed ovals in (b) encircle TI contributions.

the TI channel is now quite strong, as is placed in evidence, for example, by events at $(\text{Ne}^{2+}-\text{Ar}^{6+})$ and $(\text{Ne}^{3+}-\text{Ar}^{5+})$ intersections. The few counts in Fig. 7(b) corresponding to total final charge less than 7 are due to double scattering events. Our resolution in the TOF- B spectrum, limited by the flight time of the Ar ion along the path length viewed by the B extractor, does not allow us to separate individual Ne charges above +3.

Cross sections were obtained from spectra such as shown in Fig. 7 following the same procedure as discussed in Sec. II A above, with one modification. Configuration II yields must be divided by the efficiency for detection of the Ne ions. Since no dependence of this efficiency on the B -extractor grid voltages, above ± 5 V, was observed, the data were reduced on the assumption that this factor was the same for *all* events in the coincidence spectrum. That is, a single overall normalization factor is sufficient to place *all* cross sections from a configuration II run on an absolute scale. The value of this factor was determined by normalizing the cross section for single projectile charge exchange from $q=4$ to $q'=3$ to the configuration I data. For this case, normal capture dominates. A test of the consistency of this procedure may be made by comparing the resulting projectile charge-changing cross sections from the coincidence data, found by summing all partial cross sections leading to the same q' , with all corresponding cross sections found from the configuration I data. This is done in Fig. 6 and shows good agreement between the two sets of data.

In Fig. 8 we show the doubly-charge-differentiated cross sections obtained at 500 eV/ q . For reasons to be discussed later, we have chosen to label single, double, and triple capture as those events which produce singly, doubly, and triply charged Ne ions, respectively. Within each of these categories the cross sections are distinguished by q' . This nomenclature is different from that used in Figs. 5 and 6, and the (p) designation is therefore removed.

III. RESULTS AND DISCUSSION

Figure 5 shows the Ar-energy dependence of the (p) cross sections. Cross sections for $q=5$ and 7 are omitted to simplify the figure, since their behavior is nearly identical to that for $q=6$ and 8. Except for $q=2$ and 3, the cross sections are very nearly energy independent over the range measured. This behavior has been seen previously by Salzborn *et al.*³⁻⁵ (SMK) for similar collisions between rare-gas collision partners at projectile energies up to 100 keV, and in collisions involving H_2 targets by Huber and Kahlert.²⁵ Our data confirm the persistence of this behavior to even lower velocities.

As discussed by many authors,²⁶ one expects charge transfer in such low-energy collisions to proceed via couplings between the entrance molecular orbital (MO), correlating to the initially neutral target and charged projectile, and MO's which correlate to an ionized target and projectile. The

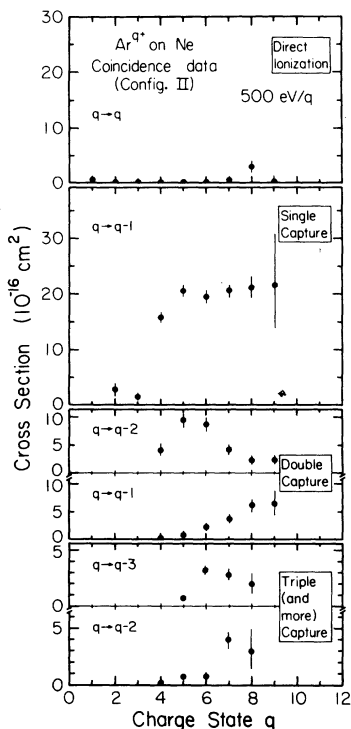


FIG. 8. Cross sections for electron capture by 500-eV/ q Ar^{q+} on Ne from configuration II data. The labels single, double, and triple and greater designate events in which the final Ne charges are +1, +2, and (+3 or greater), respectively. Within each such classification, cross sections are further differentiated according to the change of the Ar charge.

latter MO's undergo long-range crossings with the entrance channel due to the Coulomb energy of the separated ions, provided they correspond to an exoergic reaction. The general explanation for the E independence of the cross section is that, for large q , so many exoergic channels are open that any velocity dependence which might be expected due to coupling to an individual charge-transfer channel is washed out in the sum over the many available channels. The absorbing sphere model of Olson and Salop (OSAS),²⁷ which implements such a picture quantitatively, predicts a nonzero but very weak E dependence of the total charge-capture cross sections for large q . For example, the OSAS model would predict that the total cross section for capture from an 8^+ projectile from a Ne target would decrease by 25% in going from 1- to 10-keV- Ar energy.

For small q , the number of available final channels which may be fed exoergically becomes sufficiently small that an individual coupling may dom-

inate and the velocity dependence characterizing that coupling appears. For example, Huber⁸ has used a Landau-Zener formalism, appropriate for the description of a two-channel coupling, to parametrize the E dependence of the capture cross section for Ar^{2+} on Ne in this velocity range. The only exoergic channel, to which he finds experimentally most of the reaction to go, correlates to the $3s^23p^5^2P^o$ ground state of the Ar^{1+} (see Figs. 9 and 10 for partial level diagrams relevant to discussions in this section). The rising velocity dependence of $\sigma_{2,1}$ in this case is presumably due to one's being below the characteristic Landau-Zener velocity for the coupling between the incident channel and that correlating to the $(3s^23p^5^2P^o, \text{Ar}^+ - 2s^22p^5^2P^o, \text{Ne}^+)$ separated atom limit.

The low cross section for $q=3$ suggests that the transfer proceeds primarily to states with a $3s^23p^4$ final configuration, rather than the barely exoergic $3s^23p^3[^4S^o]3d$. Crossing of the incident channel with states of the former type would occur at smaller internuclear distances for $q=3$ than for the corresponding cross with $3s^23p^5$ for $q=2$, thus leading to a smaller cross section for $q=3$ than for $q=2$. For $q \geq 4$ the number of exoergically available excited states on the residual Ar ion grows rapidly and the velocity dependence of the cross sections disappears. We may therefore study the q dependence of the cross section by plotting, in Fig. 6, their velocity-averaged values. (For $q=2$ and 3, values corresponding to the high-energy plateaus in Fig. 5 were taken.) Our values are seen to be in good agreement with those of SMK at much higher energies. The sudden increase in the single (p) capture cross section at $q=4$ we attribute to the onset of transfer to the $n=4$ shell in the residual Ar ion. At this value of q , transfer to $3s^23p^2[^3P]4s$ states becomes exoergic (Fig. 10). The parent Ar^{4+} ion is $3s^23p^2^3P$, and the coupling should be strong.

For large q , several theoretical formulations, all based on a one-electron model for the multielectron target, are available. In Fig. 6 we compare our results with the following: (a) The semiclassical transfer model discussed by Ryufuku *et al.*,²⁸ Beyer *et al.*,⁹ and Mann *et al.*¹⁰ The transfer is assumed to occur at a crossing between the incident channel and the final channel characterized by a single-electron orbiting the (point) projectile core with principal quantum number n . The preferred crossing is that with the highest n for which the electron may classically surmount the potential barrier between charge centers at the crossing radius. The

Each of the above models is developed on the basis of a point charge interacting with a one-electron target. The target structure enters only through its first ionization potential. Since the models cannot distinguish between single and multiple transfer, we compare them with our total transfer cross sections in Fig. 6. The agreement between theory and data is, at best, rough. To our knowledge, no treatment has been made which explicitly deals with low-energy transfer from targets with more than two electrons to highly charged projectiles.

The coincidence data reveal two major features of capture by LEHQ ions not seen in the configuration I data.

(1) Direct ionization is so weak at these energies as to be almost undetectable in our experiment ($< 2\%$ of the single capture cross section). An exception to this appears for $q = 8$. We believe this strange behavior to be due to the presence of the metastable states $2p^5 3s^3 P_{0,2}$ in the Ar^{8+} beam. Such ions bear sufficient electronic energy into the collision that, after even single capture, the resulting ion may quickly autoionize and give rise to Ar^{8+} ions exiting from the collision region. This behavior was found to be consistently present with targets of He, Ar, Kr, and Xe, as well as Ne, and lead us to conclude that the Ar^{8+} beam bears a metastable component of about 14% which accounts entirely for the apparent rise in the direct ionization cross section at $q = 8$.

(2) Transfer ionization is an important channel for large q . This process occurs at the energetic expense of the electronic energy available from the transfer, in contrast to ionization which occurs commonly at high bombarding energies at the expense of the kinetic energy of the projectile. As discussed by other authors,^{11,12,30} several forms of transfer ionization are possible, and our experiment does not distinguish among them. We believe, however, that the most natural form of transfer ionization to occur in the collisions discussed here is through the population, in the transfer of two (or more) electrons, of doubly (or multiply) excited states on the final Ar ion.¹³⁻¹⁵ These states would autoionize after the collision, thus raising the projectile charge one (or more) unit(s) above that characterizing the primary reaction product.

Cross sections for [double capture, ($q \rightarrow q - 1$)] and [triple capture, ($q \rightarrow q - 2$)] shown in Fig. 8 are of the TI type. Since we believe that these events are most likely to come from autoionizing projectiles, and not ionization of the Ne, we assign the

single-, double-, and triple-capture labels in this figure according to the Ne charge state. The onset of TI in the double-capture case is seen to occur around $q = 6-7$. We believe this rough threshold occurs at that value of q for which sufficient energy becomes available from the transfer process to populate doubly excited, autoionizing states on the Ar core with two $4s$ electrons (see Fig. 10). Using configuration-average energies calculated with the Froese Fisher Hartree-Fock (FFHF) program,³¹ we found that the population of the final Ar configuration $3s^n 3p^m 4s^2$ becomes exoergic for q above 6. This supports our interpretation of the origin of these events. We note, however, that there seems to be considerable uncertainty as to the excitation energy of the doubly excited states for highly ionized argon. For example, the FFHF program gives an excitation energy for the singly excited $3s 3p 4s$ configuration in Ar^{7+} which is about 21 eV higher than that listed in Moore's Tables³² (see Fig. 10). Thus, the actual double excitation energy might be substantially less than that given by the program which would open the TI channel under discussion at a somewhat lower value of q . For q below 5, the program gives excitation energies in good agreement with the tables. We cannot exclude experimentally other TI mechanisms proceeding either through doubly excited Ne states or autoionization from the molecule during the collision. Both are energetically possible for q well below 6, however, and would not be expected to show the same quasithreshold behavior.

The TI process apparently feeds an important fraction of double capture cross sections back into the single (p) cross section for large q . For example, for $q = 7$, about 25% of the single (p) cross section comes through the TI double-capture channel. Since no theory exists which distinguishes between single and multiple capture from multielectron targets, the importance of TI has not yet had the opportunity to confound the comparison of theory and experiment. An exception to this may occur for the two-electron He target, where theoretical work is available. Here it will be important to isolate experimentally the TI channels before comparing with theory. We will report results similar to those given here, but for a He target, in a forthcoming article.

In summary, we have measured cross sections for electron capture and ionization by LEHQ Ar^{9+} ions colliding with Ne in a velocity regime somewhat lower than has been previously studied. Two experimental methods were used. The first allowed

us to obtain projectile charge-changing cross sections only. These we found, for q above 3, to be nearly velocity independent and to be in satisfactory agreement with published results at higher velocities. The second method allowed us to distinguish experimentally among normal capture, direct ionization, and transfer ionization, the last of which was found to be strong for q above 6. By comparing the results from the two methods we found that, by looking at the final charge states of the projectile only, one may be lead to interpret erroneously, as single capture, events that probably come from double capture followed by autoionization of the projectile. We also found that direct

ionization of the target by the incoming LEHQ Ar ions is negligible in this low-collision-energy regime.

ACKNOWLEDGMENTS

This work was supported by the Division of Chemical Sciences, U.S. Department of Energy. One of us (E.J.) acknowledges financial support from Conselho Nacional de Desenvolvimento Científico e Tecnológico (CNPq/Brasil). We thank W. C. Hammil for his assistance in the data taking.

*Present address: Battelle Northwest, Richland, Washington 99352.

- ¹See D. Crandall, R. Olson, E. Salzborn, A. Müller, F. J. de Heer, M. Panov, H. Ryufuku, T. Watanabe, R. McCarroll, and P. Valiron, in *Electron Capture by Multiply Charged Ions*, in *Invited Papers and Progress Reports of the Eleventh ICPEAC, Kyoto, 1979*, edited by N. Oda and K. Takayanagi (North-Holland, Amsterdam, 1980), p. 387.
- ²D. M. Meade, *Nucl. Fusion* **14**, 289 (1974); H. Vernickel and J. Bohdansky, *ibid.* **18**, 1467 (1978).
- ³E. Salzborn and A. Müller, in *Invited Papers and Progress Reports of the Eleventh ICPEAC, Kyoto, 1979*, edited by N. Oda and K. Takayanagi (North-Holland, Amsterdam, 1980), p. 407.
- ⁴A. Müller and E. Salzborn, *Phys. Lett.* **62A**, 391 (1977).
- ⁵H. Klinger, A. Müller, and E. Salzborn, *J. Phys. B* **8**, 230 (1975).
- ⁶D. H. Crandall, R. A. Phaneuf, and F. W. Meyer, *Phys. Rev. A* **22**, 379 (1980).
- ⁷R. Vane, M. H. Prior, and R. Marrus, *Phys. Rev. Lett.* **46**, 107 (1981).
- ⁸B. A. Huber, *J. Phys. B* **13**, 809 (1980).
- ⁹H. F. Beyer, K. -H. Schartner, and F. Folkmann, *J. Phys. B* **13**, 2459 (1980).
- ¹⁰R. Mann, F. Folkmann, and H. F. Beyer, *J. Phys. B* **14**, 1161 (1981); R. Mann, H. F. Beyer, and F. Folkmann, *Phys. Rev. Lett.* **46**, 646 (1981).
- ¹¹A. Niehaus, *Comments At. Mol. Phys.* **9**, 153 (1980); and references cited therein.
- ¹²K. C. Kulander and J. S. Dahler, *J. Phys. B* **8**, 460 (1979).
- ¹³I. P. Flaks, G. N. Ogurtsov, and N. V. Fedorenko, *Zh. Eksp. Teor. Fiz.* **41**, 1438 (1961) [*Sov. Phys.—JETP* **14**, 1027 (1962)].
- ¹⁴P. H. Woerlee, T. M. El Sherbini, F. J. de Heer, and F. W. Saris, *J. Phys. B* **12**, L235 (1979).
- ¹⁵G. N. Ogurtson, V. M. Mikoushkin, and I. P. Flaks,

Electronic and Atomic Collisions, in Abstracts of the Eleventh ICPEAC, Kyoto, 1979, edited by K. Takayanagi and N. Oda (The Society for Atomic Collision Research, Kyoto, Japan, 1979), p. 650.

- ¹⁶R. Morgenstern, A. Niehaus, and G. Zimmermann, *J. Phys. B* **13**, 4811 (1980).
- ¹⁷W. Groh, A. Müller, C. Achenbach, A. Schlachter, and E. Salzborn, *Phys. Lett.* **84A**, 77 (1981).
- ¹⁸C. L. Cocke, R. DuBois, T. J. Gray, E. Justiniano, and C. Can, *Phys. Rev. Lett.* **46**, 1671 (1981).
- ¹⁹C. L. Cocke, R. DuBois, T. J. Gray, and E. Justiniano, *IEEE Trans. Nucl. Sci.* **NS-28**, 1032 (1981).
- ²⁰C. L. Cocke, *Phys. Rev. A* **20**, 749 (1979).
- ²¹T. J. Gray, C. L. Cocke, and E. Justiniano, *Phys. Rev. A* **22**, 849 (1980).
- ²²I. A. Sellin, C. R. Vane, S. B. Ellston, J. P. Forester, P. M. Griffin, D. J. Pegg, R. S. Thoe, K. -O. Groenweld, R. Lambert, and F. Chen, *Z. Phys. A* **283**, 329 (1977).
- ²³MKS Instruments, Inc., Burlington, Mass.
- ²⁴S. K. Allison, *Rev. Mod. Phys.* **30**, 1137 (1958).
- ²⁵B. A. Huber and H. J. Kahlert, *J. Phys. B* **13**, L159 (1980).
- ²⁶See, e.g., R. Olson, in *Invited Papers and Progress Reports of the Eleventh ICPEAC*, edited by N. Oda and K. Takayanagi (North-Holland, Amsterdam, 1980), p. 391.
- ²⁷R. E. Olson and A. Salop, *Phys. Rev. A* **14**, 579 (1976).
- ²⁸H. Ryufuku, K. Sasaki, and T. Watanabe, *Phys. Rev. A* **21**, 745 (1980).
- ²⁹T. P. Grozdanov and R. K. Janev, *Phys. Rev. A* **17**, 880 (1978).
- ³⁰L. M. Kishinevskii and E. S. Parilis, *Zh. Eksp. Teor. Fiz.* **55**, 1932 (1968) [*Sov. Phys.—JETP* **28**, 1020 (1969)].
- ³¹C. Froese Fisher, *Comput. Phys. Commun.* **1**, 151 (1969).
- ³²C. E. Moore, *Natl. Bur. Stand. (U.S.) Circular No. 467* (U.S. GPO, Washington, D.C., 1952).